Biochemistry and Biophysics Reports 6 (2016) 124–134

Contents lists available at ScienceDirect

Biochemistry and Biophysics Reports

journal homepage: www.elsevier.com/locate/bbrep

Conformational features of the *Staphylococcus aureus* AgrA-promoter interactions rationalize quorum-sensing triggered gene expression

Kalagiri Rajasree, Aneesa Fasim, Balasubramanian Gopal *

Molecular Biophysics Unit, Indian Institute of Science, Bangalore 560012, India

ARTICLE INFO

Article history:
Received 11 December 2015
Received in revised form
3 March 2016
Accepted 21 March 2016
Available online 23 March 2016

Keywords:
Transcription activation
Quorum sensing
Signal Transduction
Two-component system

ABSTRACT

The intracellular trigger for the quorum sensing response mechanism in *Staphylococcus aureus* involves the phosphorylation of the response regulator AgrA by the membrane anchored histidine kinase AgrC. AgrA activates transcription from three promoter sequences (P1–P3). The promoter strength, conditional association of AgrA with these promoter elements and temporal delay in AgrA-mediated changes in gene expression contribute to the diversity of the quorum sensing response in different *S. aureus* strains. AgrA promoters comprise of imperfect direct repeats of DNA with a consensus sequence- [TA][AC][CA]GTTN [AG][TG]. Here we describe crystal structures of the DNA-binding (LytTR) domain of AgrA with different cognate DNA sequences that reveal a hitherto unanticipated feature of AgrA-DNA interactions. AgrA promoter interactions are asymmetric with fewer interactions at the binding site proximal to the −35 promoter element. Biochemical assays to evaluate AgrA-promoter interactions suggests that phosphorylation induced dimerization of AgrA can compensate for the asymmetry in AgrA-DNA interactions. The structures also provide a basis to rationalize mutations that were noted to alter AgrA activity without affecting protein-DNA interactions. Put together, the structural data, gene expression and mutational analysis reveal that promoter strength and AgrA phosphorylation enable quorum-sensing triggered transcriptional changes leading to a transition from the persistent to virulent phenotype.

1. Introduction

The accessory gene regulator mechanism (Agr) coordinates the expression of cytolytic toxins with a quorum stimulus in *Staphylococcus aureus*. The Agr quorum sensing system comprises of four components- the histidine kinase AgrC, a response regulator AgrA and a permease AgrB that processes AgrD to generate the auto-inducing peptides (AIP) that vary in sequence (AIP I-IV) [1]. AIP binding to the ecto-domain of AgrC triggers an intracellular signal transduction cascade that couples a quorum stimulus with a transcriptional response. The response regulator AgrA governs transcriptional re-engineering by binding cognate DNA sequences leading to the up-regulation or repression of gene expression. AgrA also modulates the expression of RNAIII, a pleiotropic effector involved in the up-regulation of exotoxins like alpha-haemolysin and thus has a direct role in the virulence and pathogenicity of *S. aureus* [2]. While genes in the *agr* operon are transcribed from the P2 promoter, RNAIII transcription is driven from the P3 promoter. The AgrA binding sites preceding these promoter elements are present in the intergenic region of the *agr* operon and the RNAIII locus. Another AgrA interacting sequence, referred to as the P1 promoter, governs the expression of *agrA*. While the P1 promoter was the first to be reported in the initial characterization of the *agr* locus, very little is known about AgrA-P1 interactions [3].

The response regulator AgrA has two domains- an N-terminal CheY-like receiver domain (residues 1-130) that is connected by a flexible linker to a DNA binding domain ($AgrA_{DBD}$: residues 138-238). The activation of the histidine kinase AgrC upon binding AIP initiates the phosphotransfer reaction from His239 of AgrC onto Asp59 of AgrA. AgrA is predominantly a monomer in solution and dimerizes upon phosphorylation [4]. This finding differs from the more common mechanism wherein a conformational change due to the exposure of a hydrophobic pocket in the receiver domain upon phosphorylation influences DNA binding [5]. The $AgrA_{DBD}$ domain (a representative of the LytTR domain family) adopts a ten-stranded β-scaffold with an interspaced α-helix and a short 3_{10} helix [6]. Transcription factors with the LytTR domains have been noted to govern virulence gene expression as well as regulate house-keeping functions in bacteria [7–11]. The LytTR domain of AgrA interacts with imperfect direct repeats of DNA with a consensus sequence- [TA][AC][CA]GTTN[AG][TG] [12]. These sequence motifs, separated by 12–13 basepairs, are located upstream of the −35 promoter element that is recognized by the RNA polymerase holoenzyme to initiate transcription. Activation by AgrA was

* Corresponding author.
E-mail address: bgopal@mbu.iisc.ernet.in (B. Gopal).

http://dx.doi.org/10.1016/j.bbrep.2016.03.012

suggested to be crucial for transcription from the P3 promoter whereas expression from the P2 promoter can occur independent of AgrA [13]. AgrA-mediated activation of transcription from the P1 promoter remains to be characterized. The crystal structure of an AgrA-DNA complex (referred to as P2_S2 in this manuscript) revealed that AgrA binding induces substantial conformational changes in the promoter DNA [6]. While this feature could not rationalize promoter strength, the structure revealed residues in AgrA that were important for DNA binding and conformational features that can influence promoter specificity. AgrA-promoter interactions are also sensitive to redox stimuli [14]. More recently, a post-transcriptional mechanism was suggested to regulate intracellular levels of AgrA. This mechanism, that involves the selective degradation of AgrA mRNA by CshA, is also likely to influence the temporal response to a quorum stimulus [15].

The structure of $AgrA_{DBD}$ in complex with promoter DNA (P2_S2) was first reported by Sidote et al. [6]. Here we describe the crystal structures of the $AgrA_{DBD}$ complexes with different DNA sequences. These structures revealed that the LytTR domain of AgrA makes fewer interactions with the DNA binding site located proximal to the −35 element of the promoter. We discuss the impact of these observations on the functional role of AgrA as an activator of gene expression. The structural and biochemical data presented in this manuscript suggest that phosphorylation induced dimerization of AgrA plays an important role in the selective enhancement of RNA polymerase occupancy at sub-optimal promoter elements.

2. Materials and methods

2.1. Cloning, expression and purification of recombinant AgrA DNA binding domain ($AgrA_{DBD}$)

$AgrA_{DBD}$ was amplified from *Staphylococcus aureus* genomic DNA using forward (5′ CCTAACATATGATCCATATGGATAATAGCGTTGAAACGATTGAATT 3′) and reverse (5′ GAACCCTCGAGTTATATTTTTTTAACGTTTCTCACCGATGCATAGCA 3′) primers. These amplicons were ligated between the *NdeI* and *XhoI* restriction enzyme sites of the pET22b expression vector. Insertion of a stop codon at the 5′ end of the reverse primer resulted in an expression construct without the poly-histidine affinity tag. The *E. coli* Rosetta (DE3)pLysS cells (Novagen, Inc.) were transformed with the plasmid containing $AgrA_{DBD}$ and grown at 37 °C in Luria broth with 100 μg/ml of ampicillin till the OD reached 0.5 at 600 nm. 0.5 mM IPTG (Isopropyl-β-D-thiogalactopyranoside, Gold Biotechnology Inc.) was used to induce over-expression of the protein and the culture was grown further for 16 h at 16 °C. All the purification steps were carried out at 4 °C. The cells were lysed by sonication in a buffer containing 20 mM sodium potassium phosphate pH 6.0, 100 mM NaCl and 2 mM PMSF. The lysate was subjected to centrifugation at 26,500 g for 45 min to remove the cell debris. The supernatant was added to a 80% saturated solution of ammonium sulphate with constant stirring for 1 h followed by centrifugation at 4850 g for 15 min. The pellet was re-suspended in a buffer containing 20 mM sodium potassium phosphate pH 6.0 and 100 mM NaCl and dialysed against the same buffer to remove excess ammonium sulphate. Ion exchange chromatography was performed on the dialysed lysate using a 5 ml in-house packed SP sepharose (GE healthcare) column pre-equilibrated with 20 mM sodium potassium phosphate pH 6.0 and 100 mM NaCl. The protein was eluted in a gradient of 0.7–1.5 M NaCl and analyzed on a 12% SDS-PAGE gel. Elution fractions containing the protein were pooled, concentrated and applied onto a Sephacryl S200 (HiPrep 16/60) size exclusion chromatography (GE healthcare) column pre-equilibrated with either buffer A (20 mM Bis-tris pH 6.0 and 100 mM NaCl) or buffer B (20 mM MES monohydrate pH 6.0 and 100 mM NaCl). The protein eluted as a monomer and the elution fractions were analyzed on a 12% SDS-PAGE gel and concentrated to 16 mg/ml using a 3 kDa MWCO amicon ultra centricon (Millipore, Inc.). The mass of the protein was confirmed by MALDI-TOF mass spectrometry.

2.2. Cloning, expression and purification of recombinant AgrA and $AgrA_{D59A}$

AgrA was amplified from *Staphylococcus aureus* spp COL genomic DNA using forward (5′ GAATCATATGATGAAAATTTTCATTTGCGAAGACGATCC 3′) and reverse (5′ GAACCCTCGAGTTATATTTTTTTAACGTTTCTCACCGATGCATAGCA 3′) primers. These amplicons were ligated between the *NdeI* and *XhoI* restriction enzyme sites of the pET28b expression vector. This clone was subsequently used as a template to generate the $AgrA_{D59A}$ mutant by site directed mutagenesis (double primer method- partially overlapping primers). *E. coli* Rosetta(DE3)pLysS cells (Novagen, Inc.) were transformed with the plasmid encoding AgrA or $AgrA_{D59A}$ and grown to an OD_{600} of 0.5 at 37 °C in Luria broth with 2.5 mg/ml of kanamycin. Over-expression of the proteins was initiated by induction with 0.5 mM IPTG (Isopropyl-β-D-thiogalactopyranoside, Gold Biotechnology Inc.) and the culture was further grown for 16 h at 18 °C. All purification steps were carried out at 4 °C. The cells were lysed by sonication in a buffer containing 20 mM HEPES pH 7.4, 300 mM KCl, 10% glycerol and 1 mM PMSF. The lysate was subjected to centrifugation at 26,500 × *g* for 45 minutes to remove the cell debris. The supernatant was incubated with His-select nickel affinity beads (Sigma-Aldrich, Co.) for one hour before loading onto a column. The protein was eluted by a gradient of imidazole (60–500 mM) in buffer containing 20 mM HEPES pH 7.4, 300 mM KCl and 10% glycerol. Subsequently, the partially purified protein was loaded onto a Sephacryl S-200 (HiPrep 16/60) column (GE Healthcare) pre-equilibrated with 20 mM HEPES pH 7.4, 300 mM KCl, 10% glycerol and 5 mM β-mercaptoethanol. The purity of the protein was analyzed on a 12% SDS-PAGE gel.

2.3. Prediction of the P1 promoter

Gene fusion analysis aided in the identification of the P1 promoter between the *PvuII* and *RsaI* restriction sites in the *agr* operon [3]. The region between these two restriction sites was used as an input sequence for the BPROM server, a web-based bacterial promoter prediction server, (Softberry, Inc., Mount Kisco, NY, USA; http://linux1.softberry.com) to map the −10 and −35 promoter elements. Based on the sequence characteristics of LytTR recognition motifs, the putative AgrA binding sites at the P1 promoter were identified (Fig. 1) and further characterized in this study [12].

2.4. Oligonucleotides for structural and biochemical studies

The oligonucleotides used for the crystallization, fluorescence anisotropy (Table S1) and surface plasmon resonance experiments (Table S2) were obtained from Sigma Aldrich, Co. The complementary oligonucleotides were mixed in equimolar ratios and annealed in a Bio-Rad MyCycler. In this step, the oligos were heated to 96 °C and temperature was gradually decreased to 4 °C with 1 °C/min fall in every cycle and stored at −20 °C until use.

2.5. Crystallization and structure determination

$AgrA_{DBD}$ (0.67 mM) was incubated with 0.8 mM of DNA for one hour at 4 °C prior to setting up crystallization experiments using the vapor diffusion method. Crystals for $AgrA_{DBD}$ with different

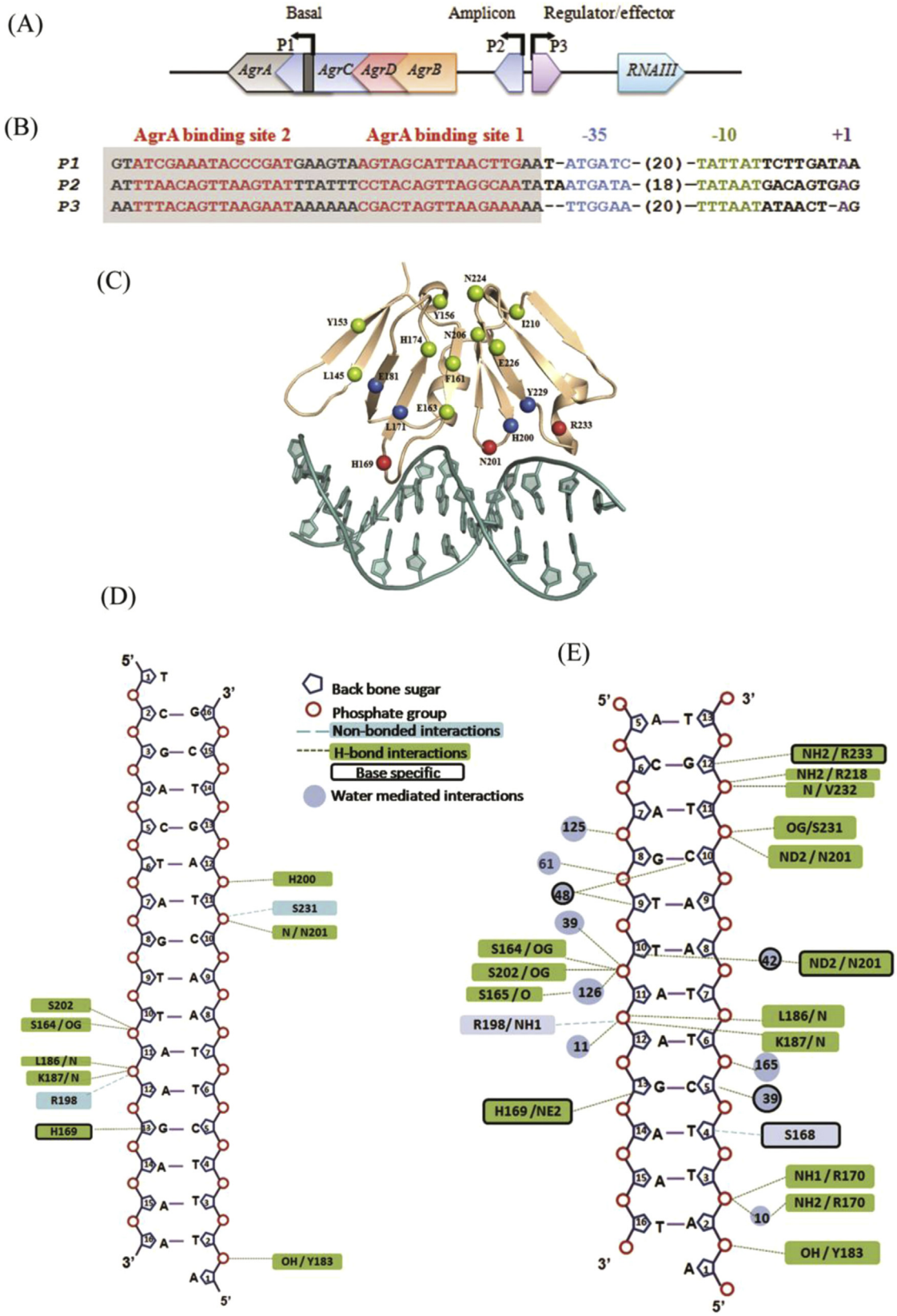

Fig. 1. The *S. aureus agr* operon. A. Schematic of *agr* operon. AgrA mediated change in gene expression occurs from three characterized promoters segments P1–P3. While P1 governs the expression of AgrA, P2 controls the expression of the entire *agr* operon. P3 dependent expression leads to up-regulation of the effector RNAIII thus providing an additional indirect mode of transcriptional re-engineering upon a quorum stimulus. B. Sequence features of P1, P2 and P3 promoter segments. The AgrA binding sites (imperfect sequence repeats) proximal and distal to transcriptional initiation site are referred to as Px_S1 and Px_S2 in the text. C. The structure of $AgrA_{DBD}$ domain in complex with the P3 promoter sites. $AgrA_{DBD}$ interacts with promoter DNA by inserting loops into two successive major grooves and an intervening minor groove. Extensive mutational analysis revealed residues which confer structural stability to the protein (green spheres) and residues which are important for protein-DNA interactions (blue spheres) [28]. The red spheres represent residues which form base specific interactions with the promoters. D. $AgrA_{DBD}$-P3_S1 promoter interactions. The P3_S1 site is seen to be less engaged in interacting with $AgrA_{DBD}$ with only one base specific interaction and few hydrogen bond interactions with the phosphate backbone. E. $AgrA_{DBD}$-P3_S2 promoter interactions. In this representation, the $AgrA_{DBD}$ is shown to be involved in three base specific interactions with P3_S2 alongside several hydrogen and non-hydrogen bonded interactions with the phosphate backbone.

promoters were obtained in various conditions (Table S3). All the crystals were grown at 18 °C. The crystals were soaked in cryo-protectant (25% Ethylene glycol) for 30 s before flash freezing in liquid nitrogen. The data were collected at the BM-14 beamline (ESRF, Grenoble) at 100 K. The diffraction images were processed using iMosflm and scaled with SCALA [16,17]. The AgrA LytTR domain promoter complex (PDB code 3BS1) was used as a search model for molecular replacement [6]. The program phaser from CCP4 suite or phenix-MR from the Phenix interface were used for the molecular replacement calculations [18,19]. The structures were refined in Refmac5 and the fit of the model to electron density was examined using COOT [20,21]. All the models were validated using MOLPROBITY and illustrative figures were prepared in PyMOL (Schrödinger, LLC) [22].

2.6. Surface Plasmon Resonance spectroscopy

The interaction kinetics of P1, P2 and P3 promoters with AgrA was analyzed by Surface Plasmon Resonance (SPR: BIACORE 2000, GE Healthcare). 5′ biotinylated promoters (Table S2) (Sigma-Aldrich, Co.) were immobilized on a Streptavidin (SA) chip (GE Healthcare). The first flow cell in the SA chip was used as a reference channel. These experiments were performed in a buffer containing 20 mM HEPES pH 7.4, 200 mM KCl, 2% glycerol and 5 mM β-mercaptoethanol. Varying concentrations of AgrA and $AgrA_{D59A}$ were used as analytes. Both AgrA and $AgrA_{D59A}$ were also incubated with 300 μM of acetyl phosphate for 30 min prior to passing on the SA chip. The binding kinetics for AgrA and $AgrA_{D59A}$ with different promoters (P1, P2 and P3) was analyzed using the BIAevaluation software (BIACORE, GE Healthcare). The rates of association and dissociation were obtained by fitting the data to a 1:1 Langmuir interaction model.

The relative specificity of AgrA for the P1, P2 and P3 promoters was evaluated using a SPR-based competition assay [23]. In this assay, biotinylated P1, P2 and P3 promoters were immobilized on a streptavidin chip (SA chip, GE Healthcare). 1 μM of AgrA was pre-incubated with 5 μM of P1, P2 and P3 promoters (non-biotinylated) at room temperature for 20 min. 1 mM acetyl phosphate was added to AgrA (1 μM) to obtain the phosphorylated protein. Both analyte samples (AgrA and AgrA pre-incubated with promoters) were evaluated for their interaction with the biotinylated promoters immobilized on the SA chip. The change in the response units due to binding of AgrA and AgrA pre-incubated with promoters were recorded. In these experiments, a competition between the immobilized promoter and a non-biotinylated promoter for AgrA results in a change in the response units. A decrease in response units can thus be correlated with stronger interactions between AgrA and the pre-incubated non-biotinylated DNA than the immobilized DNA on the chip.

2.7. Bacterial strains and growth conditions

Strains and plasmids used in this study are listed in Table 2. Cloning and DNA manipulations were performed in *E. coli* DH5α whereas *E. coli* DC10B (a DNA cytosine methyltransferase deficient strain) was used as a primary recipient for plasmids to be electroporated in to *S. epidermidis* TU3298 using a Biorad MicroPulser following the protocol reported by Augustin et al. earlier [24,25]. While *E. coli* strains were grown on LB (Luria Bertani) agar or broth at 37 °C with shaking containing 100 μg/ml ampicillin, *S. epidermidis* cells with plasmids were grown on TSB (tryptic soy) agar or broth at 37 °C with shaking containing 10 μg/ml chloramphenicol and induced with 1.0 μg/ml of anhydrotetracycline (ATC).

2.8. GFP reporter plasmid construction

pRMC2 (an *E. coli* - Staphylococci shuttle vector) has one multiple cloning site between *KpnI* and *EcoRI* restriction sites. For GFP reporter plasmid assays, an additional cloning site was introduced between *PstI* and *HindIII* by the addition of a *NheI* restriction site. This modified pRMC2 vector is referred to as pRMC2M in this study. *Agr* P1, P2 and P3 promoters were amplified from *S. aureus* COL genome using the primers tabulated in Table S4. GFP was amplified from the pKEN vector using primers (GFP_P1_Fw, GFP_P2_Fw, GFP_P3_Fw and GFP_Nhe_Rv). Overlap extension PCR was used to fuse the promoters with the GFP and the resulting PCR product was digested with *PstI* and *NheI* restriction enzymes and ligated into the cloning site-2 of pRMC2M (P1GFP, P2GFP and P3GFP clones).

2.9. Cloning and site directed mutagenesis of agrA

S. aureus agrA was amplified using primers AgrA_Fw and AgrA_Rv. The amplified product was digested with *KpnI* and *EcoRI* restriction enzymes (cloning site 1) and ligated into the pRMC2M vector with P1GFP, P2GFP or P3GFP cloned at the cloning site 2. Clones were confirmed by sequencing. A single primer was used for site directed mutagenesis in which P1GFP-AgrA, P2GFP-AgrA and P3GFP-AgrA clones were used as templates (Table S4). The PCR product was treated with *DpnI* for 2 h at 37 °C before transforming into *E. coli* DH5α. Three other plasmid clones were used as controls. These had only P1GFP, P2GFP and P3GFP at cloning site 2 and a vacant cloning site 1 (no *agrA*). All the reporter plasmid clones were confirmed by sequencing.

2.10. RNA isolation and qRT-PCR reaction

0.5 ml of *S. epidermidis* cells, uninduced and induced (with ATC) were harvested after 3 hours of growth. Two volumes of RNA protect reagent (Qiagen) was added to *S. epidermidis* cells and incubated for 10 minutes at room temperature before centrifugation at 7000 rpm for 10 min at 4 °C. These cells were stored at −80 °C till further use. RNA was isolated from *S. epidermidis* using previously described protocols [26]. Cells were thawed on ice and resuspended in 500 μl of acidified phenol chloroform (5:1) pH 4.5 (Ambion) and mixed with 500 μl of NAES buffer (50 mM sodium acetate pH 5.1, 10 mM EDTA, 1% SDS) at room temperature. The sample was transferred to tubes containing 0.1 mm zirconia-silica beads and vortexed (4800 rpm × 30 s × 2times) with intermittent incubation on ice using a mini bead beater (Biospec, inc.). After this step, the tubes were centrifuged at 12,000 × *g* for 5 minutes at 4 °C. Around 450 μl supernatant was precipitated with 520 μl of isopropanol and 35 μl of 3 M sodium acetate. The pellet was washed with 70% ethanol and the tubes were completely dried before resuspending in 25 μl of RNase free water. RNA samples were treated with RNase-free DNase (Qiagen) for 1 hour at 37 °C and RNA was further purified using RNAeasy mini kit (Qiagen) before cDNA synthesis. 1 μg of RNA was converted to cDNA using iscript reverse transcription supermix (Biorad, Inc.). 20 ng of cDNA per reaction was used for quantitative real time PCR (qRT-PCR) with the Biorad iQ5 thermo cycler. The primers used to amplify target genes are listed in Table S5. The reaction mixtures were incubated for 3 min at 95 °C, followed by 40 cycles of 30 s at 95 °C, 30 s at 52 °C, and 30 s at 72 °C and a final extension at 72 °C for 5 min. The chloramphenicol acetyl transferase (*cat*) gene which is an antibiotic marker of pRMC2 plasmid was used both as an endogenous control as well as to monitor the copy number of the plasmid per cell. The relative transcription levels of target genes were determined by the $2^{-\Delta\Delta_{ct}}$ method by using the values from uninduced samples as control [27]. The values represent the mean standard deviation from three independent experiments.

3. Results and discussion

3.1. Comparison of the AgrA LytTR domain promoter DNA complexes

AgrA influences transcription from three promoter elements (P1–P3) (Fig. 1A). Each promoter comprises of imperfect direct repeats referred to as binding site 1 (proximal to −35 promoter element) and binding site 2 (distal to −35 promoter element) in this manuscript (Fig. 1B). The distal site (Site 2) is located 12 bp upstream of site 1. Crystal structures of the $AgrA_{DBD}$ in complex with these different promoter DNA sequences were determined to evaluate conformational features that enable transcriptional activation. While all three pairs of $AgrA_{DBD}$ complexes (corresponding to the DNA sequences at the P1, P2 and P3 elements) could be crystallized, crystals of the $AgrA_{DBD}$-P1 complexes diffracted poorly in comparison to the P2 and P3 complexes. The structural comparisons were thus limited to four structures- corresponding to the P2 (P2_S1 and P2_S2) and the P3 promoter sequences (P3_S1 and P3_S2). The diffraction data, refinement and model statistics for these structures are compiled in Table 1.

$AgrA_{DBD}$ belongs to the LytTR family of response regulator proteins with ten β-strands assuming a β-β-β fold. Unlike other DNA binding proteins, $AgrA_{DBD}$ interactions with DNA are governed by residues located in the loop segments of the protein (Fig. 1C). These interactions comprise of both direct and indirect readouts involving base specific interactions as well as interactions with the phosphodiester backbone. The structures of both apo and DNA bound $AgrA_{DBD}$ have been described earlier [6]. However, a comparison between the structures of $AgrA_{DBD}$ bound to different DNA complexes revealed a pattern to AgrA-DNA interactions that was hitherto unanticipated. A common element in all four $AgrA_{DBD}$-DNA complexes is a direct readout between the Guanine 13 on Strand A in the major groove with His169 and nine indirect readouts formed through hydrogen bonding and van der Waals interaction with the phosphodiester backbone. Apart from these interactions, the site 2 of both P2 and P3 promoters formed two more base specific interactions with the DNA. These include Asn201 interacting with Thymine 10 (Strand A) in P3_S2 and Agr233 which makes electrostatic interactions with Guanine 12 (Strand B) in both P3_S2 and P2_S2 (Fig. S1). The residues present in the loops form about 12–16 interactions with the phosphodiester backbone at the site 2 of P2 and P3 promoters. A comparison between the pairs of site 1 and site 2 complexes however, revealed an interesting pattern in the protein-DNA interactions (Fig. 2). The AgrA binding site proximal to the −35 element ($AgrA_{DBD}$:P2_S1; $AgrA_{DBD}$:P3_S1) has fewer protein-DNA interactions than the distal interacting segment ($AgrA_{DBD}$:P2_S2; $AgrA_{DBD}$:P3_S2) (Figs. 1D, S2 and S3). These enhanced interactions in case of AgrA with the binding site distal to the transcription start site suggest a role for this site in anchoring the AgrA dimer.

The crystal structures also rationalize mutations that were noted to substantially influence AgrA activity. These residues were classified as those that abrogate DNA binding, residues that influence protein stability and point mutants that influence transcription activation (Figs. 1C and S4) [28]. For example, His200 which was shown to affect protein DNA interactions (apart from His169, Arg233 and Asn201 which were shown to distort $AgrA_{DBD}$-P2_S2 promoter interactions by Sidote et al.), forms a hydrogen bond with the phosphate backbone of the P3_S1 promoter DNA. In P2_S1, His200 forms interactions with deoxyribose sugar while in P2_S2, a water molecule coordinates this interaction with the phosphate backbone. The AgrA LytTR domain-promoter complex (referred to as P2_S2 in this study) introduces a 35° bend in the conformation of the bound DNA [6]. In the four complexes that were examined, a distortion of 30–36° was observed except in the case of the P2_S1 promoter where the conformational change is

Table 1
Diffraction data and refinement statistics.

	Native (PDB: 4XYO)	P2_S1 promoter (PDB: 4XXE)	P2_S2 promoter (PDB: 4XYQ)	P3_S1 promoter (PDB: 4XQQ)	P3_S2 promoter (PDB: 4XQJ)	P3_S2 promoter (PDB: 4XQN)
Diffraction Data						
Wavelength (Å)	0.97625	0.95372	1.54179	0.97625	0.95372	0.95372
Space group	$P22_12_1$	$P4_2$	$P4_1$	C121	C121	P1
Cell dimensions a, b, c (Å) α, β, γ (deg)	31.27, 45.67, 95.45	97.03, 97.03, 51.11	47.77, 47.77, 100.25	79.02, 145.60, 62.10 β=93.09	91.03, 92.87, 45.15 β=98.59	45.17, 61.32, 64.1 α=91.09 β=97.48 γ=94.02
Resolution (Å)	45.03–2.0 (2.25–2.0)#	68.42–3.2 (3.32–3.20)	50.12–2.4 (2.49–2.40)	62.01–3.05 (3.26–3.05)	35.02–1.9 (2.0–1.9)	44.69–2.3 (2.38–2.3)
[a]R_{sym} (%)	8.4 (66.9)	12.6 (110.3)	8.1 (46.1)	9.6 (82.5)	6.5 (66.2)	10.0 (56.0)
I/σI	14.3 (3.4)	14.1 (1.2)	9.6 (2.9)	6.9 (1.34)	12.6 (2.1)	6.9 (2.7)
CC(1/2)	0.99 (0.92)	0.99 (0.70)	0.996 (0.89)	0.99 (0.90)	0.99 (0.77)	0.99 (0.8)
No. of unique reflections	9581 (669)	8040 (777)	8820 (838)	13,297 (2408)	29,281 (2957)	29,349 (2898)
Multiplicity	12.3 (11.8)	14.8 (15.6)	4.2 (4.5)	3.8 (3.8)	4.4 (4.4)	3.9 (3.9)
Completeness (%)	98 (91.8)	99.96 (100)	99.7 (100.0)	99.3 (99.4)	100 (100)	97.1 (96.3)
Refinement						
[b]R_{cryst}	19.3	29.6	20.1	26.13	18.8	21.1
[c]R_{free}	23.3	33.9	23.8	30.5	22.5	24.7
No. of residues/solvent/ligand	99/77/5	254/0/0	135/22/4	460/0/0	247/166/25	491/95/9
Model Ramachandran Statistics						
Preferred (%)	96.9	96	97.0	97	96.4	99
Allowed (%)	3.1	3.0	3.0	3.0	3.6	1.0
Outliers (%)	0	1	0	0	0	0
R.m.s. Deviations						
Length (Å)	0.009	0.011	0.012	0.009	0.011	0.012
Angle (°)	1.34	1.49	1.61	1.33	1.54	1.64

Values in the parenthesis represent the outer resolution shell statistics

[a] $R_{sym}=\Sigma_{hkl}\ \Sigma_i\ |I_i(hkl)-<I(hkl)>|/\Sigma_{hkl}\ \Sigma_i\ I_i(hkl)$, where $I_i(hkl)$ is the intensity of the i^{th} reflection $<I(hkl)>$ is the average intensity.

[b] $R_{cryst}=\Sigma_{hkl}||F_{obs}|-|F_{calc}||/\Sigma_{hkl}|F_{obs}|$.

[c] R_{free} was calculated as for R_{cryst} but using 5% of the data that were excluded from the refinement calculation.

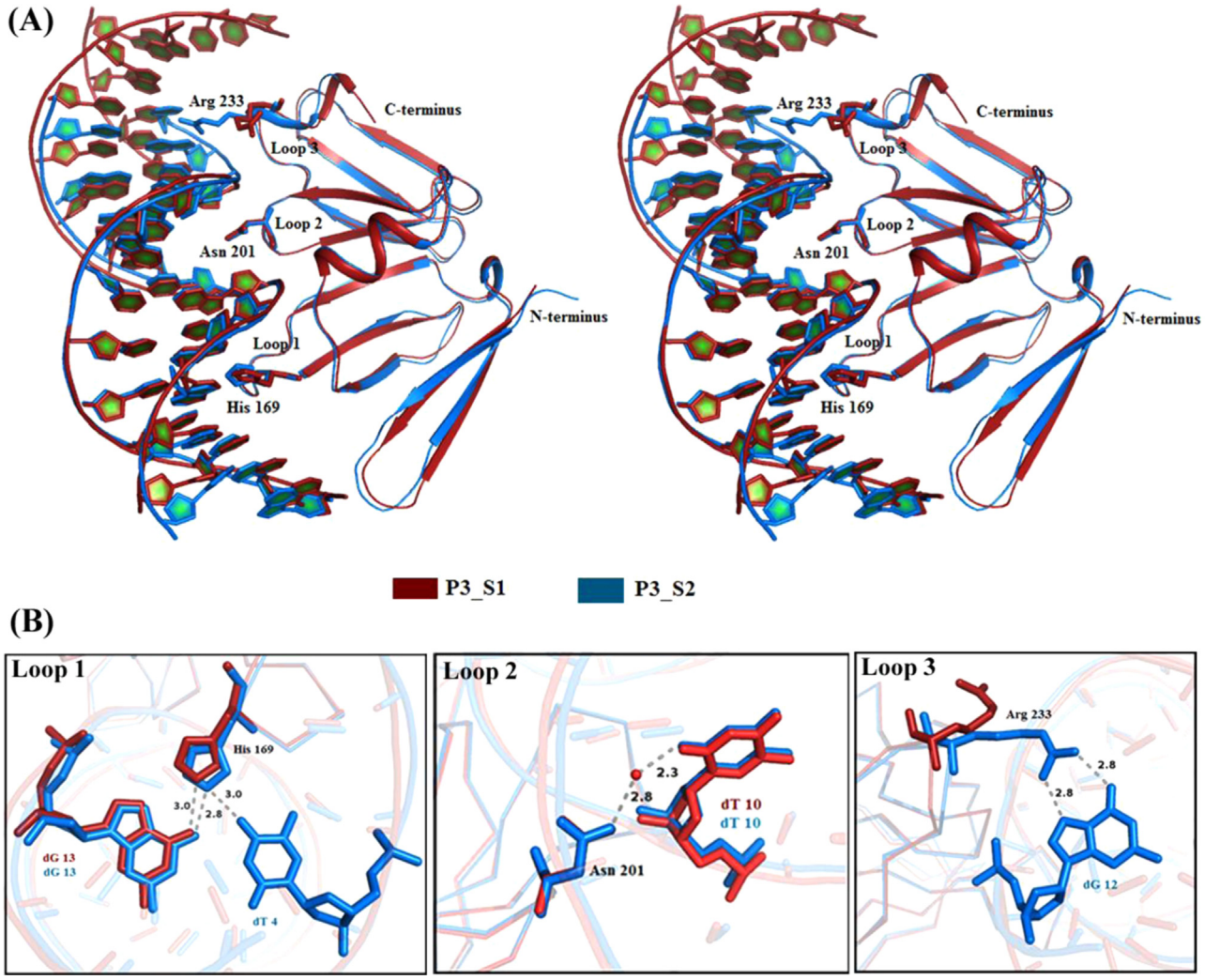

Fig. 2. Structural features of $AgrA_{DBD}$-promoter interactions. (A) Stereo representation of the $AgrA_{DBD}$-promoter interactions. (B) The residues which are involved in base specific interactions are superimposed. The structures of the $AgrA_{DBD}$ complex with the P3_S1 and P3_S2 promoters reveal that P3_S1 interactions involve fewer protein DNA contacts that P3_S2.

Table 2
Bacterial strains and plasmids.

Bacterial Strains/Plasmids	Description	Reference
Bacterial Strains		
E. coli DH5α	F^2 (w80d DlacZ M15) D(lacZYA-argF) U169 hsdR17(r2M) recA1endA1 relA1 deoR12 phoA supE44 thi-1, gyrA96	[31]
E. coli DC10B	Δdcm in the DH10B background, Dam methylation only	[24]
S. aureus COL	Clinical isolate, genomic DNA	[32]
S. epidermidis TU3298	Capable of being transformed with and stably maintaining recombinant plasmids.	[25]
Plasmids		
pRMC2	Derivative of the tetracycline-inducible expression vector pALC2073; anhydrotetracycline inducible expression vector, Amp^r in E.coli, Chl^r in *S. aureus.*	[33]
pRMC2M	pRMC2 vector with cloning site 2 after TetR gene having (*Pst1, Sph1, Mfe1,Nhe1* and *HindIII*) restriction site.	This Study
P1GFP-AgrA	AgrA in cloning site 1 with *agr*P1 promoter driven GFP, cloned in cloning site 2 of pRMC2M.	This Study
P2GFP-AgrA	AgrA in cloning site 1 with *agr*P2 promoter driven GFP, cloned in cloning site 2 of pRMC2M.	This Study
P3GFP-AgrA	AgrA in cloning site 1 with *agr*P3 promoter driven GFP, cloned in cloning site 2 of pRMC2M.	This Study
P1GFP-$AgrA_{D59A}$	$AgrA_{D59A}$ in cloning site 1 with *agr*P1 promoter driven GFP, cloned in cloning site 2 of pRMC2M.	This Study
P2GFP-$AgrA_{D59A}$	$AgrA_{D59A}$ in cloning site 1 with *agr*P2 promoter driven GFP, cloned in cloning site 2 of pRMC2M.	This Study
P3GFP-$AgrA_{D59A}$	$AgrA_{D59A}$ in cloning site 1 with *agr*P3 promoter driven GFP, cloned in cloning site 2 of pRMC2M.	This Study
P1GFP-ΔAgrA	*agr*P1 promoter driven GFP, cloned in cloning site 2 of pRMC2M.	This Study
P2GFP-ΔAgrA	*agr*P2 promoter driven GFP, cloned in cloning site 2 of pRMC2M.	This Study
P3GFP-ΔAgrA	*agr*P3 promoter driven GFP, cloned in cloning site 2 of pRMC2M.	This Study

much lower (25.9° global bend over a 13 bp stretch calculated using Curves+[29]). Indeed, the buried surface area for P2_S1 is only 1293 $Å^2$ when compared to other AgrA LytTR-promoter complexes that have a larger interacting interface 1400–1500 $Å^2$) [30]. The variations noted in the crystal structures of $AgrA_{DBD}$ with different promoter complexes suggest a mechanism whereby the

Table 3
Interaction between AgrA and cognate DNA sequences monitored by Surface Plasmon Resonance spectroscopy.

	P1 promoter			P2 promoter			P3 promoter		
	k_a (X 10^{+4} M^{-1} s^{-1})	k_d (X 10^{-3} s^{-1})	K_D (X 10^{8} M)	k_a (X 10^{+4} $M^{-1}s^{-1}$)	k_d (X 10^{-3} s^{-1})	K_D (X 10^{-8} M)	k_a (X 10^{+4} M^{-1} s^{-1})	k_d (X 10^{-3} s^{-1})	K_D (X 10^{-8} M)
AgrA	1.24	2.38	19.2	1.61	1.06	6.59	1.32	2.02	15.3
AgrA∼P	1.54	1.53	9.92	2.76	1.11	4.02	7.05	1.47	2.09
$AgrA_{D59A}$	1.16	1.93	16.6	2.24	1.60	7.14	1.99	2.13	10.7
$AgrA_{D59A}$∼P	1.07	1.33	12.4	1.45	1.11	7.68	1.26	1.33	10.5

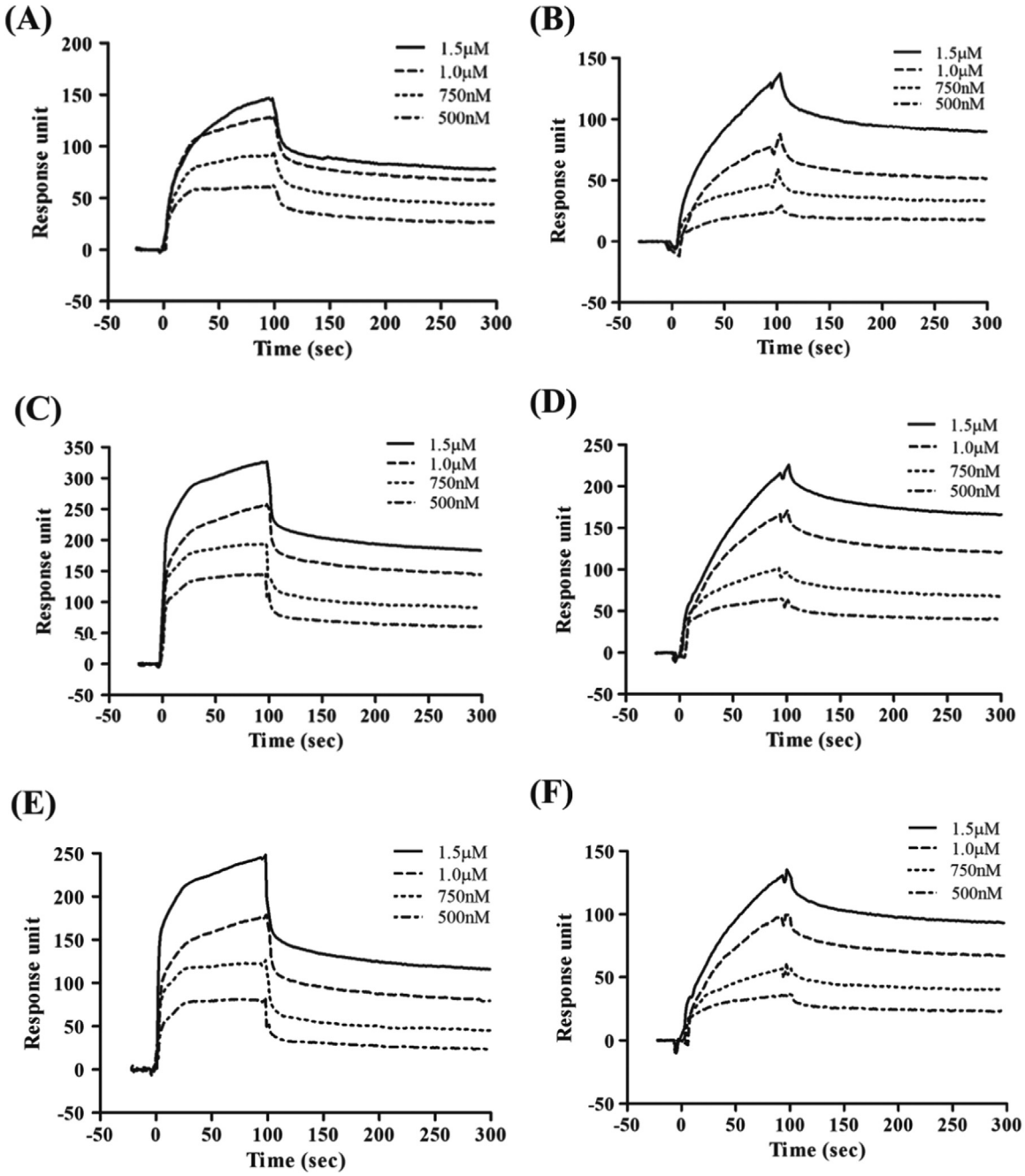

Fig. 3. Relative affinity between AgrA and the P1, P2 and P3 promoter binding sites. Protein DNA interactions monitored by SPR. Varying concentrations of AgrA were passed onto an Streptavidin chip with **(A)** P1 **(C)** P2 and **(E)** P3 promoters to ascertain the relative affinity. The role of phosphorylation of AgrA on **(B)** P1 **(D)** P2 and **(F)** P3 were also analyzed. In these experiments, phosphorylation was noted to alter AgrA P3 interactions more substantially than the others (Table 2).

imperfect direct repeats in the promoter sequences could influence AgrA function (Table 2).

In the light of earlier reports wherein AgrA was also demonstrated to be redox-sensitive, several attempts were made to obtain the oxidized form of this protein. However, in all the structures that were determined in this study, we could not

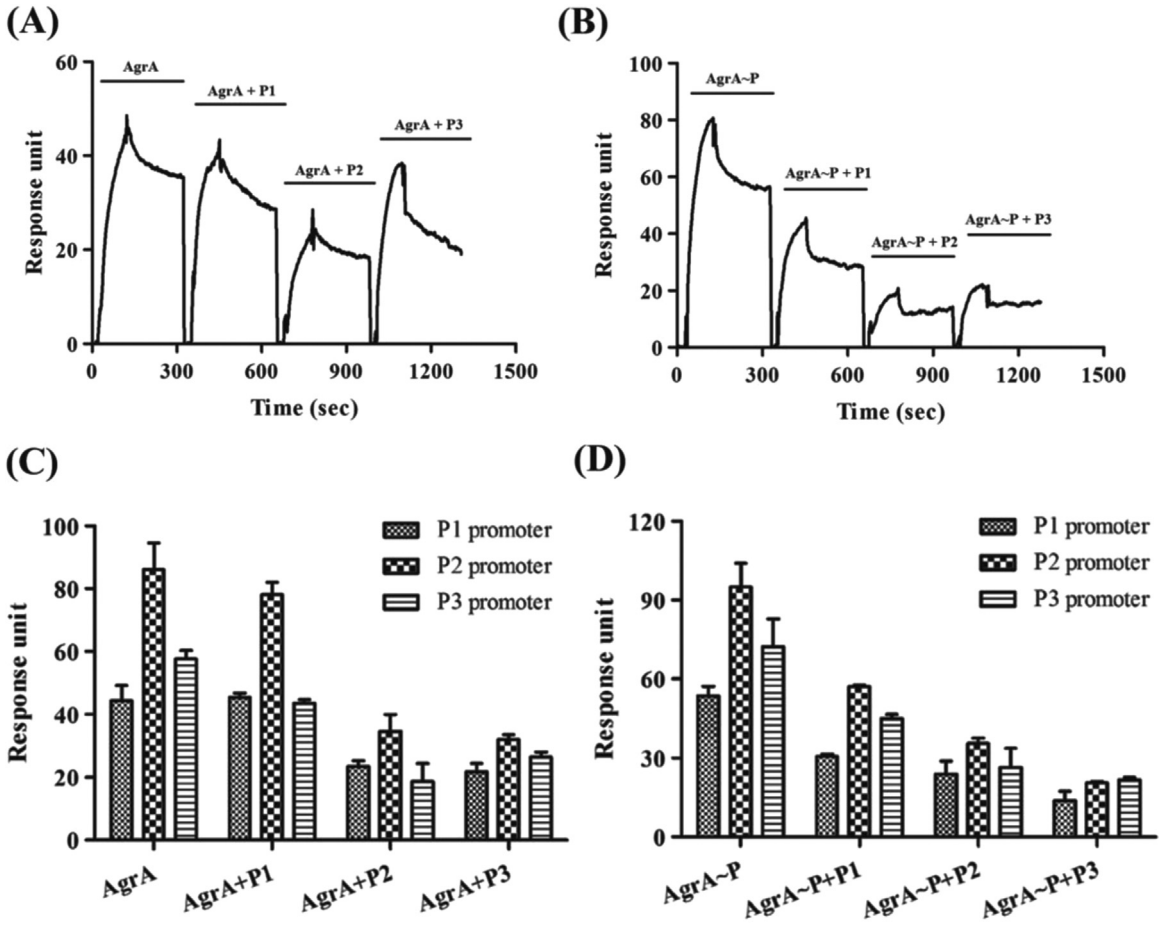

Fig. 4. Relative promoter affinity evaluated by SPR. The relative affinity of P1, P2 and P3 promoters were evaluated by a competition assay. **A.** AgrA or AgrA pre-incubated with P1, P2 and P3 promoters (non-biotinylated) served as an analyte in these experiments. The P3 promoter DNA was immobilized on the sensorgram. The relative change in the response units upon incubation of AgrA with promoters suggests that P2 has higher affinity for AgrA than P3 and P1 promoters (P2 > P3 > P1). **B.** A similar experiment was repeated with phosphorylated AgrA where a change in affinity was observed (P3 > P2 > P1). **C.** An illustrative representation of change in the response units resulting from the competition between the immobilized biotinylated promoters with non-biotinylated promoters for AgrA and phosphorylated AgrA (**D**).

observe electron density corresponding to the disulfide in the LytTR domain. Based on the structure of apo-AgrA and mutational analysis, it appears that the disulfide could substantially distort the domain conformation, thus limiting protein-DNA interactions under oxidising conditions (Fig. S5).

3.2. *Promoter strength determines the stringency of AgrA- induced expression changes*

The affinity of AgrA for different promoter sequences was examined using Surface Plasmon Resonance (SPR) experiments. In the SPR experiments, the promoter DNA was immobilized using a streptavidin tag. Both phosphorylated and non-phosphorylated forms of AgrA served as an analyte in these studies. The sensorgrams of phosphorylated AgrA interaction with promoters were fit to Langmuir 1:1 model. The fits were validated by both residual values which range from −10 to +10 with chi square values within 10. The association (k_a) and dissociation (k_d) constants along with the equilibrium dissociation constant (K_D) values for the three promoter sequences are compiled in Table 3. The strength of interaction of AgrA with P2 promoter is more than P1 and P3 promoters. The effect of phosphorylation of Asp59 (upon addition of acetyl phosphate) is more prominent in case of the P3 promoter (~7 times) compared to the P1 and P2 promoters where the affinity increased less than two fold (Fig. 3 and Table 3). The affinity for AgrA is twice in the case of P3 when compared to P2 upon phosphorylation. The active site mutant $AgrA_{D59A}$ does not show considerable difference in affinity between the phosphorylated and non-phosphorylated protein (Fig. S6 and Table 3). The specific nature of these interactions was evaluated using a DNA segment corresponding to the intergenic region of 31 base pairs between the P2 and P3 binding sites. This DNA sequence did not show any interaction with AgrA or the dimeric phosphorylated protein.

To further examine the relative affinity for different promoter elements, AgrA-promoter interactions were also examined by a competitive binding assay using SPR (Figs. 4 and S7). In these experiments, the biotinylated promoter DNA was immobilized on the SPR chip. The relative change in the response units upon the passage of AgrA pre-incubated with the unlabelled promoter DNA was monitored. This competition assay suggests that AgrA binds more efficiently to the P2 than the P1 and P3 promoter sequences with the order P2 > P3 > P1 (Fig. 4A and C). In another experiment AgrA was pre-incubated with acetyl phosphate and unlabelled promoter 30 min prior to the SPR experiment. When AgrA was incubated with unlabelled promoter in presence of acetyl phosphate and passed onto the SPR chip, the change in response units was lower suggesting that AgrA (phosphorylated) bound the unlabelled P3 promoter more tightly when compared to the other immobilized promoters. The order of affinity is changed to P3 > P2 > P1 upon phosphorylation (Fig. 4B and D).

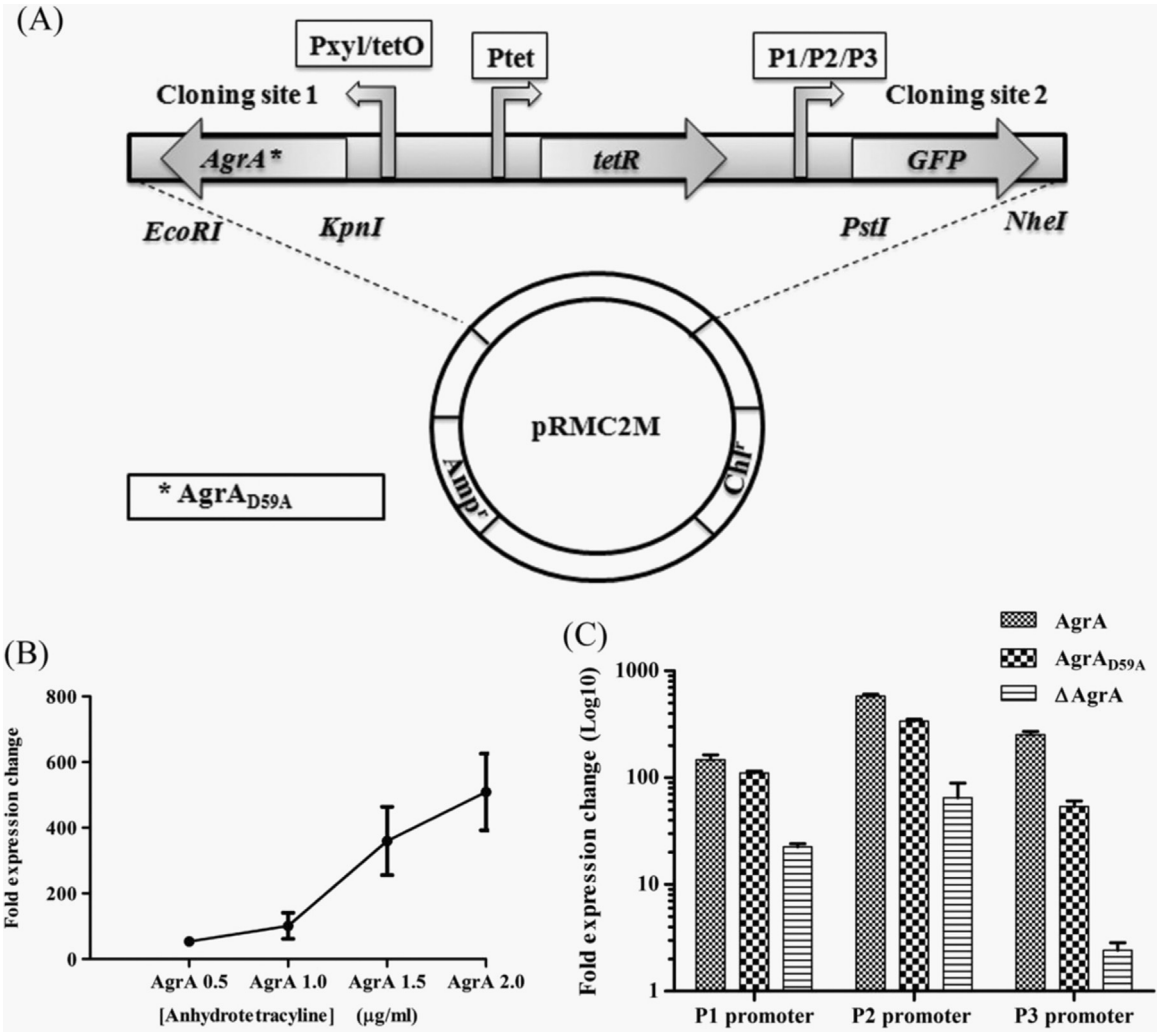

Fig. 5. Variations in promoter strength define AgrA induced changes in the transcriptional profile. A. Schematic of the plasmid employed to evaluate promoter strength. B. qRT-PCR analysis of AgrA induced expression changes. The linear change in AgrA expression upon induction provides a basis to evaluate AgrA induced GFP expression under the control of promoters. C. Three variants of AgrA (AgrA, $AgrA_{D59A}$ and ΔAgrA) induced with anhydrotetracycline. The fold expression change in GFP at a fixed AgrA concentration was examined for the P1, P2 and P3 promoters. As reported earlier, P2 dependent expression levels are substantially higher. The qRT-PCR data suggest that P3 dependent changes are more influenced by AgrA phosphorylation.

3.3. Role of AgrA in RNA polymerase recruitment

The finding that the binding affinity of $AgrA_{DBD}$ for the P1, P2 and P3 promoter sequences are similar suggested that other parameters are likely to account for the diversity in AgrA induced changes in the expression profile. The influence of phosphorylation was evaluated using a cellular assay based on green fluorescent protein (GFP) markers (Fig. 5A). The premise for this experiment is that an increase in the intracellular concentration of AgrA would change the expression of genes that are located downstream of the P1, P2 or P3 promoter element. As this assay relies on the change in intracellular concentration of AgrA upon the addition of the inducer anhydrotetracycline (ATC), this aspect was verified by qRT-PCR (Fig. 5B). The $AgrA_{D59A}$ mutant that lacked the aspartate residue involved in phosphorylation served as a 'constitutively inactive' AgrA in these experiments. Changes in the expression levels of GFP under the control of P1, P2 and P3 promoter segments were examined at a similar AgrA concentration (fixed ATC concentration). The consequent change in GFP expression was examined by quantitative real-time PCR analysis (qRT-PCR analysis) (Fig. 5C). The qRT-PCR data revealed that GFP expression under the control of the P2 promoter is substantially higher than P1 or P3 promoters (Fig. 5). This finding *per se* is not surprising given that the spacing between the −35 and −10 elements in the P2 promoter is more optimal (18 bp) than either P1 or P3 (where the spacing is 20 bp) (Fig. 1B). We also note that the expression of GFP under both P1 and P2 promoter elements did not vary between AgrA and the $AgrA_{D59A}$ mutant. However, the change in GFP expression under the P3 promoter was substantially different between that induced by AgrA and the non-phosphorylated $AgrA_{D59A}$ mutant (Fig. 5C). Similar results were obtained when the GFP fluorescence was measured by flow cytometry (Fig. S8). Put together, this finding suggests that non-phosphorylated AgrA can retain constitutive expression of *AgrA* and the *agr* operon. The release of secreted toxins as well as changes in expression by the RNAIII effector (that rely on the P3 promoter), however, are selectively enhanced upon AgrA phosphorylation.

Previous studies on the transcription of the agr operon revealed that the transcription competent open promoter complex (RPo) occurs more readily at P2 than at P3 [13]. This suggested a potential role for AgrA in RNA polymerase recruitment with the caveat that AgrA selectively increases the occupancy of the RNA polymerase at a promoter site depending on the cellular context. The mechanism that would enable this mode of AgrA mediated transcription initiation remained unclear. Here we propose a

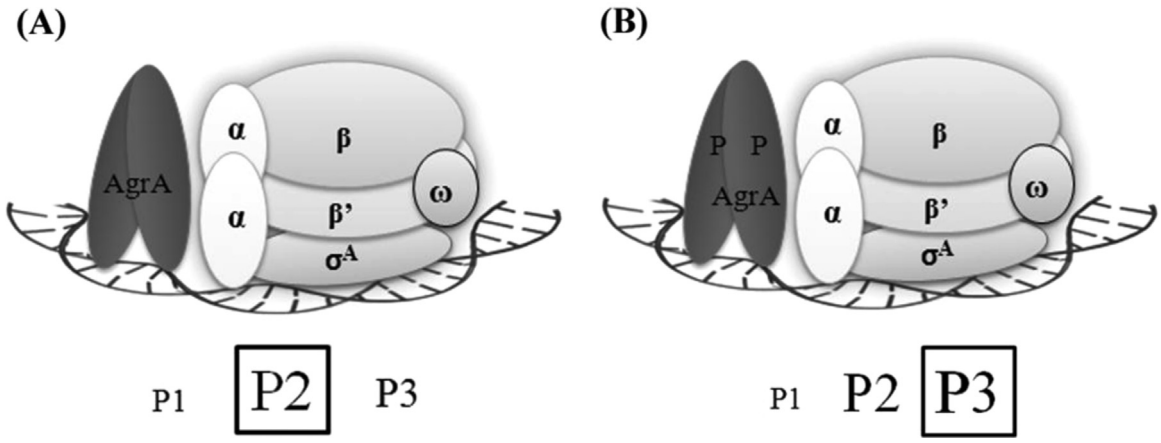

Fig. 6. A mechanistic model for AgrA dependent transcriptional re-engineering. Intracellular AgrA exists in both the phosphorylated and non-phosphorylated forms. The non-phosphorylated AgrA governs basal AgrA expression and by extension that of the *Agr* operon from the P2 promoter. Phosphorylation alters promoter specificity resulting in higher RNAIII levels and expression of toxin genes with consequent physiological changes.

mechanistic model based on biochemical data as well as the asymmetry in AgrA-promoter interactions noted from the crystal structures of the AgrA-DNA complexes (Fig. 6). *In vitro* biochemical assays as well as a competition assay to evaluate promoter selection reveal that AgrA binds more efficiently to the P2 than the P1 or P3 promoters. Phosphorylation affects this complex in distinct ways. Previous studies revealed that AgrA dimerization is stronger upon phosphorylation [4]. Here we note that phosphorylation substantially influences AgrA binding to the P3 promoter. AgrA-P1 as well as AgrA-P2 interactions are relatively less affected by AgrA phosphorylation. Another relevant observation is that the P3 promoter is sub-optimal (20 bp spacing between the –35 and −10 promoter elements) when compared to the P2 promoter. A comparison between transcription activation by phosphorylated AgrA and the $AgrA_{D59A}$ mutant shows that GFP expression under the control of the P3 promoter is selectively enhanced upon AgrA phosphorylation. Put together, these observations support the hypothesis that the phosphorylated AgrA dimer improves RNA polymerase recruitment at the sub-optimal P3 promoter thus enhancing the expression of toxin genes. The model thus provides a link between AgrA phosphorylation and the virulent phenotype of *S. aureus* that is characterized by increased levels of intracellular RNAIII as well as secreted toxins.

4. Conclusion

A comparison between the crystal structures of $AgrA_{DBD}$ with different promoters and biochemical data on AgrA-promoter interactions suggest a mechanism that can rationalize the role of AgrA as an activator of gene expression. These studies suggest that the level of exotoxins in *S. aureus* is regulated by locating these genes under a sub-optimal promoter that is selectively enhanced upon AgrA activation by a quorum stimulus.

Author contributions

KR, AF and BG designed the studies, KR and AF performed the experiments, KR, AF and BG analyzed the experiments. KR and BG wrote the manuscript.

Acknowledgements

This study was supported by a grant (SR/SO/BB-0125/2010) from the Department of Science and Technology, India. The Center for Infectious Disease Research is partially funded by a grant from the Infosys Foundation. Access to the BM-14 beamline at ESRF is funded by a grant from the Department of Biotechnology, India.

The PDB accession codes for the deposited structures are 4XQJ, 4XQN, 4XQQ, 4XXE, 4XYO and 4XYQ.

Appendix A. Supporting information

Supplementary data associated with this article can be found in the online version at http://dx.doi.org/10.1016/j.bbrep.2016.03.012.

References

[1] L. Zhang, L. Gray, R.P. Novick, G. Ji, Transmembrane topology of AgrB, the protein involved in the post-translational modification of AgrD in Staphylococcus aureus, J. Biol. Chem. 277 (2002) 34736–34742, http://dx.doi.org/10.1074/jbc.M205367200.

[2] S. Boisset, T. Geissmann, E. Huntzinger, P. Fechter, N. Bendridi, M. Possedko, et al., Staphylococcus aureus RNAIII coordinately represses the synthesis of virulence factors and the transcription regulator Rot by an antisense mechanism, Genes. Dev. 21 (2007) 1353–1366, http://dx.doi.org/10.1101/gad.423507.

[3] H.L. Peng, R.P. Novick, B. Kreiswirth, J. Kornblum, P. Schlievert, Cloning, characterization and sequencing of an accessory gene regulator (agr) in Staphylococcus aureus, J. Bacteriol. 170 (1988) 4365–4372.

[4] S.K. Srivastava, K. Rajasree, A. Fasim, G. Arakere, B. Gopal, Influence of the AgrC-AgrA complex on the response time of Staphylococcus aureus quorum sensing, J. Bacteriol. 196 (2014) 2876–2888, http://dx.doi.org/10.1128/JB.01530-14.

[5] P.G. Leonard, D. Golemi-Kotra, A.M. Stock, Phosphorylation-dependent conformational changes and domain rearrangements in Staphylococcus aureus VraR activation, Proc. Natl. Acad. Sci. USA 110 (2013) 8525–8530, http://dx.doi.org/10.1073/pnas.1302819110.

[6] D.J. Sidote, C.M. Barbieri, T. Wu, A.M. Stock, Structure of the Staphylococcus aureus AgrA LytTR domain bound to DNA reveals a beta fold with an unusual mode of binding, Structure 16 (2008) 727–735, http://dx.doi.org/10.1016/j.str.2008.02.011.

[7] J.K. Cheung, J.I. Rood, The VirR response regulator from Clostridium perfringens binds independently to two imperfect direct repeats located upstream of the pfoA promoter, J. Bacteriol. 182 (2000) 57–66, http://dx.doi.org/10.1128/JB.182.10.2992–2992.2000.

[8] R.L. Koenig, J.L. Ray, S.J. Maleki, M.S. Smeltzer, B.K. Hurlburt, Staphylococcus aureus AgrA binding to the RNAIII-agr regulatory region, J. Bacteriol. 186 (2004) 7549–7555, http://dx.doi.org/10.1128/JB.186.22.7549–7555.2004.

[9] O. Ween, P. Gaustad, L.S. Håvarstein, Identification of DNA binding sites for ComE, a key regulator of natural competence in Streptococcus pneumoniae, Mol. Microbiol. 33 (1999) 817–827, http://dx.doi.org/10.1046/j.1365–

2958.1999.01528.x.
[10] D.P. Miller, J.R. Frederick, J. Sarkar, R.T. Marconi, The Treponema denticola AtcR LytTR domain-containing response regulator interacts with three architecturally distinct promoter elements: implications for understanding the molecular signaling mechanisms that drive the progression of periodontal disease, Mol. Oral. Microbiol. 29 (2014) 219–232, http://dx.doi.org/10.1111/omi.12059.
[11] P.A. Risøen, O. Johnsborg, D.B. Diep, L. Hamoen, G. Venema, I.F. Nes, Regulation of bacteriocin production in Lactobacillus plantarum depends on a conserved promoter arrangement with consensus binding sequence, Mol. Genet. Genom. 265 (2001) 198–206, http://dx.doi.org/10.1007/s004380000397.
[12] A.N. Nikolskaya, M.Y. Galperin, A novel type of conserved DNA-binding domain in the transcriptional regulators of the AlgR/AgrA/LytR family, Nucleic Acids Res. 30 (2002) 2453–2459, http://dx.doi.org/10.1093/nar/30.11.2453.
[13] J. Reynolds, S. Wigneshweraraj, Molecular insights into the control of transcription initiation at the staphylococcus aureus agr operon, J. Mol. Biol. 412 (2011) 862–881, http://dx.doi.org/10.1016/j.jmb.2011.06.018.
[14] F. Sun, H. Liang, X. Kong, S. Xie, H. Cho, X. Deng, et al., Quorum-sensing AGR Mediates Bacterial Oxidation Response via an Intramolecular disulfide Redox Switch in the Response regulator AgrA, Proc. Natl. Acad. Sci. 109 (2012) 9095–9100, http://dx.doi.org/10.1073/pnas.1200603109.
[15] S. Oun, P. Redder, J.-P. Didier, P. François, A.-R. Corvaglia, E. Buttazzoni, et al., The CshA DEAD-box RNA helicase is important for quorum sensing control in Staphylococcus aureus., RNA Biol. 10 (2013) 157–165, http://dx.doi.org/10.4161/rna.22899.
[16] T.G.G. Battye, L. Kontogiannis, O. Johnson, H.R. Powell, A.G.W. Leslie, iMOSFLM: A new graphical interface for diffraction-image processing with MOSFLM, Acta Crystallogr. Sect. D Biol. Crystallogr. 67 (2011) 271–281, http://dx.doi.org/10.1107/S0907444910048675.
[17] M.D. Winn, C.C. Ballard, K.D. Cowtan, E.J. Dodson, P. Emsley, P.R. Evans, et al., Overview of the CCP4 suite and current developments, Acta Crystallogr. Sect. D Biol. Crystallogr. 67 (2011) 235–242, http://dx.doi.org/10.1107/S0907444910045749.
[18] A.J. McCoy, R.W. Grosse-Kunstleve, P.D. Adams, M.D. Winn, L.C. Storoni, R. J. Read, Phaser crystallographic software, J. Appl. Crystallogr. 40 (2007) 658–674, http://dx.doi.org/10.1107/S0021889807021206.
[19] P.D. Adams, P.V. Afonine, G. Bunkóczi, V.B. Chen, I.W. Davis, N. Echols, et al., PHENIX: A comprehensive Python-based system for macromolecular structure solution, Acta Crystallogr. Sect. D Biol. Crystallogr. 66 (2010) 213–221, http://dx.doi.org/10.1107/S0907444909052925.
[20] G.N. Murshudov, P. Skubák, A.A. Lebedev, N.S. Pannu, R.A. Steiner, R. A. Nicholls, et al., REFMAC5 for the refinement of macromolecular crystal structures, Acta Crystallogr. Sect. D Biol. Crystallogr. 67 (2011) 355–367, http://dx.doi.org/10.1107/S0907444911001314.
[21] P. Emsley, K. Cowtan, Coot: Model-building tools for molecular graphics, Acta Crystallogr. Sect. D Biol. Crystallogr. 60 (2004) 2126–2132, http://dx.doi.org/10.1107/S0907444904019158.
[22] V.B. Chen, W.B. Arendall, J.J. Headd, D.A. Keedy, R.M. Immormino, G.J. Kapral, et al., MolProbity: all-atom structure validation for macromolecular crystallography, Acta Crystallogr. Sect. D Biol. Crystallogr. 66 (2010) 12–21, http://dx.doi.org/10.1107/S0907444909042073.
[23] H.F. Teh, W.Y.X. Peh, X. Su, J.S. Thomsen, Characterization of protein-DNA interactions using surface plasmon resonance spectroscopy with various assay schemes, Biochemistry 46 (2007) 2127–2135, http://dx.doi.org/10.1021/bi061903t.
[24] I.R. Monk, I.M. Shah, M. Xu, M.W. Tan, T.J. Foster, Transforming the untransformable: application of direct transformation to manipulate genetically Staphylococcus aureus and Staphylococcus epidermidis, MBio (2012), http://dx.doi.org/10.1128/mBio.00277-11.
[25] J. Augustin, F. Götz, Transformation of Staphylococcus epidermidis and other staphylococcal species with plasmid DNA by electroporation, FEMS Microbiol. Lett. 54 (1990) 203–207.
[26] S.J. Vandecasteele, W.E. Peetermans, R. Merckx, J. Van Eldere, Quantification of expression of Staphylococcus epidermidis housekeeping genes with Taqman quantitative PCR during in vitro growth and under different conditions, J. Bacteriol. 183 (2001) 7094–7101, http://dx.doi.org/10.1128/JB.183.24.7094–7101.2001.
[27] M.W. Pfaffl, A new mathematical model for relative quantification in real-time RT-PCR, Nucleic Acids Res. 29 (2001) e45, http://dx.doi.org/10.1093/nar/29.9.e45.
[28] S.S. Nicod, R.O.J. Weinzierl, L. Burchell, A. Escalera-Maurer, E.H. James, S. Wigneshweraraj, Systematic mutational analysis of the LytTR DNA binding domain of Staphylococcus aureus virulence gene transcription factor AgrA, Nucleic Acids Res. 42 (2014) 12523–12536.
[29] R. Lavery, M. Moakher, J.H. Maddocks, D. Petkeviciute, K. Zakrzewska, Conformational analysis of nucleic acids revisited: Curves+, Nucleic Acids Res. 37 (2009) 5917–5929, http://dx.doi.org/10.1093/nar/gkp608.
[30] E. Krissinel, K. Henrick, Inference of macromolecular assemblies from crystalline state, J. Mol. Biol. 372 (2007) 774–797, http://dx.doi.org/10.1016/j.jmb.2007.05.022.
[31] D. Hanahan, Studies on transformation of Escherichia coli with plasmids, J. Mol. Biol. 166 (1983) 557–580, http://dx.doi.org/10.1016/S0022-2836(83)80284-8.
[32] S.R. Gill, D.E. Fouts, G.L. Archer, E.F. Mongodin, R.T. DeBoy, J. Ravel, et al., Insights on evolution of virulence and resistance from the complete genome analysis of an early methicillin-resistant Staphylococcus aureus strain and a biofilm-producing methicillin-resistant Staphylococcus epidermidis strain, J. Bacteriol. 187 (2005) 2426–2438, http://dx.doi.org/10.1128/JB.187.7.2426–2438.2005.
[33] R.M. Corrigan, T.J. Foster, An improved tetracycline-inducible expression vector for Staphylococcus aureus, Plasmid 61 (2009) 126–129, http://dx.doi.org/10.1016/j.plasmid.2008.10.001.